Transnational University Limburg is a unique collaboration of two universities in two countries: the University of Hasselt and Maastricht University.

UHASSELT
KNOWLEDGE IN ACTION

www.uhasselt.be
Universiteit Hasselt
Campus Hasselt:
Martelarenlaan 42 | 3500 Hasselt
Campus Diepenbeek:
Agoralaan Gebouw D | 3590 Diepenbeek

UHASSELT
KNOWLEDGE IN ACTION

Maastricht University

Faculty of Medicine and Life Sciences
School for Life Sciences
Master of Biomedical Sciences

Master's thesis

Highlighting the Potential of Cold Atmospheric Plasma Therapy in Reducing the Growth of Cancer-Derived 3D Organoids

Sara Esbati

Thesis presented in fulfillment of the requirements for the degree of Master of Biomedical Sciences, specialization Molecular Mechanisms in Health and Disease

SUPERVISOR :
Prof. dr. Annelies BRONCKAERS

SUPERVISOR :
Dr. Angela PRIVAT MALDONADO

MENTOR :
Ms. Jana BAROEN

2024
2025

UHASSELT
KNOWLEDGE IN ACTION

Maastricht University

Faculty of Medicine and Life Sciences
School for Life Sciences
Master of Biomedical Sciences

Master's thesis

Highlighting the Potential of Cold Atmospheric Plasma Therapy in Reducing the Growth of Cancer-Derived 3D Organoids

Sara Esbati

Thesis presented in fulfillment of the requirements for the degree of Master of Biomedical Sciences, specialization Molecular Mechanisms in Health and Disease

SUPERVISOR :
Prof. dr. Annelies BRONCKAERS

SUPERVISOR :
Dr. Angela PRIVAT MALDONADO

MENTOR :
Ms. Jana BAROEN

Highlighting the Potential of Cold Atmospheric Plasma Therapy in Reducing the Growth of Cancer-Derived 3D Organoids*

Sara Esbati[1], Jana Baroen[2,3,4], and Angela Privat Maldonado[2,3]

[1] Faculty of Medicine and Life Sciences, Department of Biomedical Sciences, Hasselt University, Hasselt, Belgium
[2]CORE, Faculty of Medicine and Health Sciences, University of Antwerp, Antwerp, Belgium
[3]PLASMANT, Faculty of Sciences, University of Antwerp, Antwerp, Belgium
[4]Environmental Intelligence Unit, Institute for Technological Research (VITO), Mol, Belgium

*Running title: *CAP-Induced Suppression of Organoid Growth*

To whom correspondence should be addressed: Dr. Angela Privat Maldonado, Tel: +32 3 265 25 76; Email: angela.privatmaldonado@uantwerpen.be

Keywords: Cold atmospheric plasma, Pancreatic ductal adenocarcinoma, Head and neck squamous cell carcinoma, Patient-derived tumor organoids, Organoid growth rate, Reactive oxygen and nitrogen species

ABSTRACT

Cancer remains a major health challenge in the 21st century. Conventional therapies still suffer from limitations, including lack of selectivity, resistance to treatment, and severe side effects. Cold atmospheric plasma (CAP), a partially ionized gas enriched with reactive species, has shown potential to address current challenges by selectively inducing oxidative stress in cancer cells. Most scientific evidence is derived from two-dimensional cell cultures, which fail to accurately capture the complexity of human tumors. However, three-dimensional organoids offer a more realistic model, preserving the heterogeneity and morphology of patient tumors. This study evaluated the impact of CAP on organoids derived from head and neck squamous cell carcinoma (HNSCC) and pancreatic ductal adenocarcinoma (PDAC) patients, which are two of the most aggressive and lethal cancers. Organoid growth was monitored using live-cell imaging, and CAP-induced reactive species were quantified using fluorometric assays. The results demonstrated that CAP exerted treatment time-dependent suppression of organoid growth, with PDAC-derived organoids displaying higher sensitivity compared to HNSCC-derived organoids. CAP also induced a treatment time-dependent increase in hydrogen peroxide and nitrite levels. Notably, hydrogen peroxide levels declined over time in the presence of organoids, suggesting active uptake, whereas nitrite levels remained relatively stable. These findings demonstrate CAP's potential to effectively target cancer cells in a more realistic tumor model and provide insights into its dynamic response across different cancer types and patient-derived organoids. Collectively, this study supports CAP application as a promising cancer therapy and highlights the relevance of organoid-based models for translational cancer research.

INTRODUCTION

Background & Problem – Cancer is derived from the Greek word *Karkinos,* meaning crab, because the veins surrounding the tumor branch out, resembling a crab's legs (1). It refers to the group of diseases characterized by uncontrolled cell proliferation and the development of metastatic properties (2). This dysregulation mainly arises from the activation of oncogenes and/or the inactivation of tumor suppressor genes, resulting in uncontrolled cell cycle progression and the suppression of apoptotic pathways (2). In light of its aggressive nature, it ranks among the most prevalent and deadly diseases worldwide (3). Based on a report published in 2020 by the International Agency for Research on Cancer, almost 19.3 million new cancer cases and 10 million cancer-related deaths were reported globally (4). Thus, cancer continues to pose a significant public health challenge worldwide (5). Among these, pancreatic ductal adenocarcinoma (PDAC) stands as the most widespread and one of the most lethal forms of pancreatic cancer, accounting for almost 90% of its cases (6). PDAC

is also known for its resistance to current therapies, contributing to its position as the seventh leading cause of cancer-related death (7, 8). One of the key contributors to this resistance is cancer cell plasticity, particularly epithelial to mesenchymal transition (EMT), which enhances cellular invasiveness and treatment evasion (7). Moreover, the hypovascular tumor microenvironment (TME), immunosuppressive behavior like natural killer cell suppression, and extensive desmoplasia further contribute to PDAC resistance to current therapies (7). Another cancer that also continues to present a considerably low five-year survival rate of 40-50% is head and neck squamous cell carcinoma (HNSCC) (9). It ranks as the sixth most prevalent malignancy globally, with approximately 900,000 new cases and over 450,000 deaths annually (10). The high mortality rate in HNSCC is partially related to its resistance mechanisms, such as the upregulation of drug efflux transporters like multidrug resistance-associated protein one, breast cancer resistance protein, and P-glycoprotein (11). These transporters actively expel antitumor agents from cancer cells, leading to diminished intracellular concentration and reduced therapeutic efficacy (11). Furthermore, they employ advanced anti-apoptotic mechanisms, including the overexpression of Bcl-2 family proteins and activation of the phosphoinositide 3-kinase/AKT/mammalian target of the rapamycin pathway, which also contributes to resistance against the treatment (12). HNSSCC TME also plays an important role in this resistance through different mechanisms such as hypoxia, altered metabolism, reduction/oxidation (redox) systems, and immune evasion (9).

Current treatment limitations – In addition to resistance mechanisms observed in cancers like PDAC and HNSCC, conventional cancer treatments, such as chemotherapy, radiotherapy, and surgery, suffer from various drawbacks - including systemic toxicity, drug resistance, adverse effects, poor pharmacokinetics, limited tumor-specific targeting, and patient burden -, despite considerable advancements in the field (3, 5). For instance, while surgery is still considered the main approach for treating PDAC patients, only 20% of patients are eligible for it (13). Additionally, in 75% of cases, cancer cells remain microscopically detectable at the primary tumor site (13). In HNSCC, radiochemotherapy, known as one of the standard treatments, is frequently associated with side effects such as leukopenia and thrombocytopenia, which heighten the risk of bleeding and infection, as well as mucositis, dermatitis, and dysphagia (14). Although immunotherapy has become a novel therapeutic approach for various cancers, only a limited number of HNSCC and PDAC patients have exhibited a positive response to it (15, 16). HNSCC and PDAC TME are enriched with dysregulated and hyperactivated fibroblasts known as cancer-associated fibroblasts (CAFs), which contribute to immunosuppression (17, 18). CAFs facilitate the recruitment of regulatory T cells, tumor-associated neutrophils, tumor-associated macrophages, and myeloid-derived suppressor cells, all of which play a critical role in promoting tumor progression, immune evasion, and resistance to immunotherapy (18-20). Additionally, the dense stroma in PDAC, which forms 80% of the tumor mass, acts as a physical barrier that hinders the delivery of immunotherapies to cancer cells (18). Accordingly, there is a growing interest in developing cancer treatments that are better tolerated, more effective, and have better selectivity towards cancer cells while being less harmful to normal cells (21).

A novel treatment approach – Among emerging therapeutic strategies, cold atmospheric plasma (CAP) has recently shown notable promise in cancer treatment (21). CAP is a partially ionized gas generated at near-room temperature by applying energy, typically in the form of an electromagnetic field, to neutral gas (22). It produces a rich cocktail of reactive oxygen and nitrogen species (RONS), charged particles, ultraviolet (UV) radiation, and localized electric fields that can trigger cellular responses that cause cell death with specific selectivity to cancer cells (23, 24). Its anticancer effects are primarily mediated through RONS, which are classified into long-lived and short-lived reactive species (25, 26). Short-lived reactive species comprise superoxide anion ($O_2^{\bullet -}$), singlet oxygen ($^1O_2$), hydroxyl radical (•OH), and peroxynitrite ($ONOO^-$), among others (18). The short-lived reactive species contribute significantly to CAP-induced cytotoxicity (25). For instance, •OH is a highly reactive oxidizing substance that plays a vital role in cell membrane disruption, DNA inhibition, lipid peroxidation, and apoptosis induction via the mitochondrial pathway (25). The long-lived reactive species encompass hydrogen peroxide (H_2O_2), nitrite (HNO_2/NO_2^-), nitrate (HNO_3/NO_3^-), etc. (27). Of these species, H_2O_2 is known as a major contributor to the

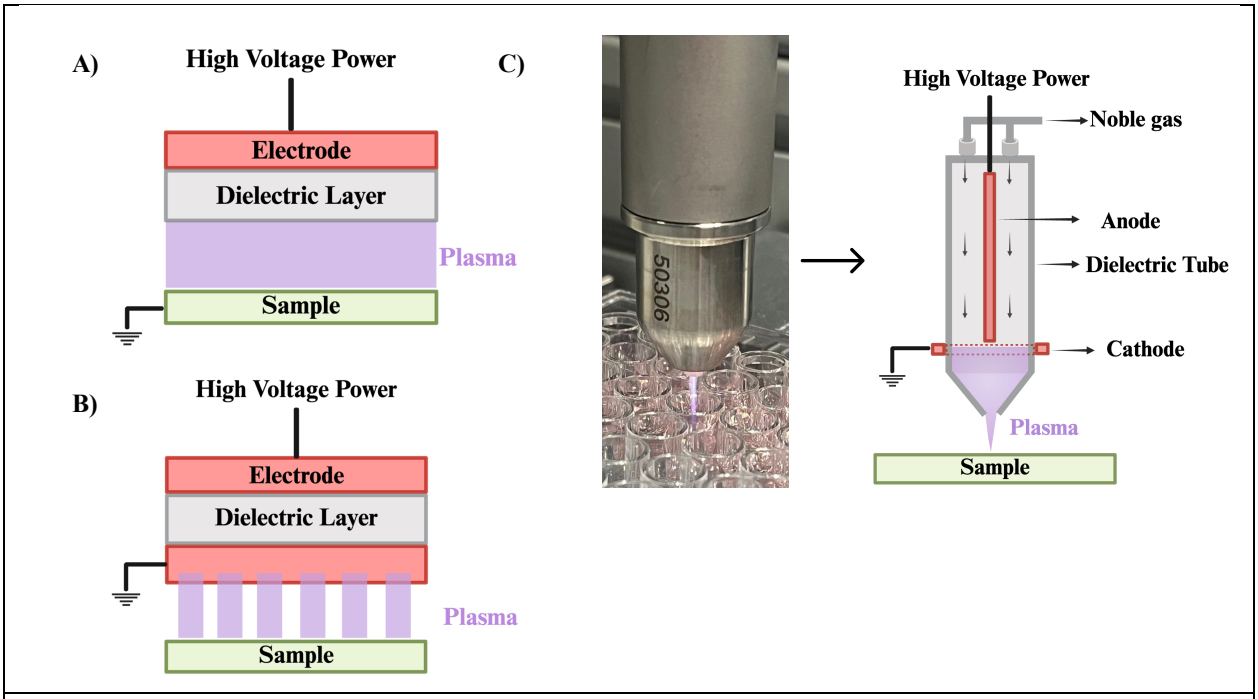

Figure. 1 – Representative CAP Sources. This figure illustrates commonly used CAP devices, including, volume DBD source (**A**), surface discharge source (**B**), and CAP jet source (**C**). Figure created with BioRender The design adapted from Yan *et al.*, 2021.

anticancer efficacy of CAP treatment (27). Yan *et al*. have demonstrated that H_2O_2 generated through CAP treatment rapidly triggers the NF-κB activation and promotes early expression of interleukin-2 and its receptor α-chain in cancer cells, ultimately initiating immune responses against them (28).

CAP generation & delivery methods – CAP can be generated through several methods, with dielectric barrier discharge (DBD) and plasma jets being the most frequently used devices in cancer therapy (29). In DBDs, plasma is generated either in the gap between the high-voltage electrode and the target, allowing direct contact with the plasma (volume DBDs), or on the surface of a specially designed electrode separated from the opposing electrode (surface DBDs) (Figure 1A and 1B)(30). On the other hand, the plasma jet generates a discharge between two electrodes while the sample remains outside of the discharge region (Figure 1C)(31). Furthermore, DBD devices typically operate in ambient air, using atmospheric air as a working gas for plasma generation (32, 33). However, plasma jets rely on an active gas flow, mainly noble gases like helium or argon, to efficiently transport active plasma species to the target (33). The use of each device depends on its intended application. For instance, the flat geometry of DBDs makes them proper for treating superficial cancerous tumors like melanoma (31). In contrast, CAP jets are particularly advantageous for targeting non-planar surfaces, enabling access to cavities, and allowing for precise, spot-like treatment (31). Furthermore, CAP delivery methods can be classified into direct and indirect strategies (34). The direct approach involves the application of CAP directly to samples, such as *in vitro* cell cultures or *in vivo* models (34). Conversely, the indirect method entails treating a physiological solution with CAP for a defined period to produce a plasma-activated liquid, such as medium, phosphate-buffered saline (PBS), deionized (DI) water, among others, which is subsequently administered to the target samples (34, 35). All the mentioned physical factors, including UV radiation, electric field, and others, as well as both short- and long-lived RONS, are involved in direct CAP treatment (36). However, the indirect approach exerts its effect on cancer cells exclusively through long-lived RONS (36).

CAP mechanisms of action – Various studies confirmed that cancer cells have higher levels of endogenous RONS compared to normal cells (5). Moreover, the expression of aquaporins (AQP), water transport channel proteins, considerably increases in cancer cells (36). Since certain AQP isoforms also facilitate the H_2O_2 transport, they represent an important pathway for H_2O_2 infiltrating cells (36). Consequently, cancer cells show greater permeability to H_2O_2 and uptake them at a higher

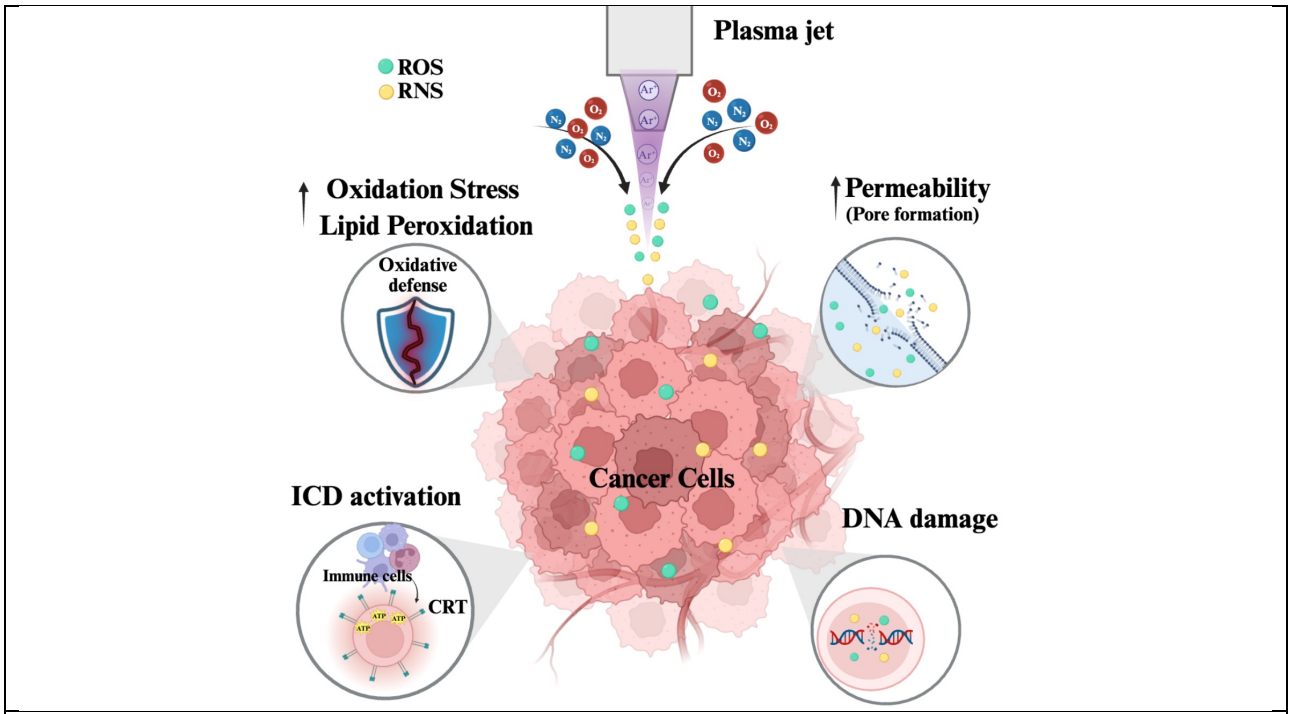

Figure. 2 – **Mechanism of action of CAP on cancer cells.** Interaction between ambient air molecules (O_2 and N_2) and highly activated particles in the CAP field leads to the generation of reactive oxygen and nitrogen species (ROS and RNS). Cancer cells, which exhibit higher membrane permeability, are more susceptible to the uptake of these reactive species. Given their already elevated basal ROS/RNS levels, the additional oxidative burden induced by CAP overwhelms cellular antioxidant defenses, leading to oxidative stress and lipid peroxidation. Furthermore, CAP treatment causes DNA damage and promotes immunogenic cell death (ICD) by inducing the release of damage-associated molecular patterns, such as adenosine triphosphate (ATP) and calreticulin (CRT). Figure generated with BioRender and inspired by Chupradit *et al.*, 2022.

rate (36). Reduced cholesterol levels in cancer cell membranes, intended to enhance membrane fluidity and plasticity to facilitate metastasis, also make these cells susceptible to reactive oxygen species (ROS)- induced oxidative stress (37, 38). This elevated vulnerability accelerates membrane lipid peroxidation, which in turn results in the formation of more pores in cell membranes, allowing for greater diffusion of RONS into the cells (Figure 2)(37). Consequently, intracellular oxidative stress exceeds the oxidative defense system and its threshold, thereby resulting in cell death (Figure 2)(39). The other proposed mechanism of tumor cell susceptibility to CAP-induced RONS is the increased replication rate of cancer cells (24). They enter the S phase of the cell cycle more frequently, during which DNA is unwound and more vulnerable to RONS (Figure 2)(24). In addition to RONS-mediated effects, other physical components of CAP, such as UV radiation and electric fields, can induce DNA damage and trigger cell cycle arrest (24). Therefore, an optimal CAP irradiation dose can selectively induce regulated cell death (RCD) in various cancer cells without causing significant damage to non-malignant surrounding tissue (24). Recent research has demonstrated that CAP also activates an antitumor immune response against cancer cells, more specifically a process called immunogenic cell death (ICD) (Figure 2)(36). ICD is a distinct form of RCD compared to apoptosis and necroptosis, for example, due to its ability to elicit antigen-mediated immune responses, which ultimately leads to the development of immunological memory (40). ICD involves modifications in the cell surface composition and the secretion of signaling molecules called damage-associated molecular patterns (DAMPs), including high-mobility group protein B1 (HMGB1), calreticulin (CRT), adenosine triphosphate (ATP), and heat shock proteins (36). DAMPs stimulate the infiltration of dendritic cells into the TME, enhance the uptake and processing of tumor antigens, and promote the efficiency of antigen presentation to T cells (41). Furthermore, it has been found that CAP induces a wide variety of post-translational modifications (PTMs) (42). PTMs play a pivotal role in governing protein structure and function by adding small chemical molecule groups to

amino acid side chains or altering existing groups (43). Therefore, CAP can cause conformational changes in protein structure and alter their functional properties (44). This can potentially modify interactions among cancer cells and the TME, ultimately diminishing tumor invasiveness and immunosuppression while enhancing the permeability of therapeutic agents (23, 43). In particular, RONS generated by CAP oxidize proteins and introduce a variety of oxidative post-translational modifications (oxPTMs) (44). Through oxPTMs, CAP could potentially expand the repertoire of tumor-specific antigens known as neoantigens and enhance the antigenicity of tumor-associated ligands and receptors (44). The presence of tumor antigens is critical for priming and activating immune cells, especially T cells (44). Additionally, by inducing oxPTMs of receptors and proteins that are present in cancer cell-extracellular environments, CAP can also reduce their tumorigenic and immunosuppressive functions (44). Yusupov *et al.* indicate that CAP can diminish the proliferative potential of cancer cells through the oxidation of hyaluronan (HA) and CD44 (45). Cancer cells commonly overexpress HA and CD44, which have a role in enhancing cancer proliferation, migration, adhesion, and inflammatory response (44). Furthermore, evidence suggests that CAP through the oxidation of CD47, an important immune checkpoint inhibitor that restrains innate immune cell activity, contributes to the reduction of cancer cell-mediated immunosuppression (46).

Research gaps – Although recent studies have demonstrated encouraging results and promising potential in using CAP for cancer treatment, most studies have been conducted on two-dimensional (2D) cell cultures, with limited research on more complex biological systems. The major limitation of 2D cell cultures is their inability to precisely replicate cancer cells *in vivo* since only rare clones can expand and sustain growth over multiple passages (47, 48). Hence, the derived cell lines may acquire remarkable genetic alterations and fail to represent the original tumor's genetic heterogeneity accurately (48). Furthermore, cell lines are mainly derived from single cells; therefore, they fail to accurately reproduce the complex and dynamic nature of tumors, which are often composed of diverse cell populations (47, 49). Notably, their 2D structure alters cell polarity, morphology, and division mechanisms, as well as disturbing interactions between the cellular and extracellular environments (47). Additionally, studies investigating PTMs in response to CAP have mainly been conducted on isolated protein solutions (50). There remains a remarkable gap in understanding how CAP affects PTMs in living cells, particularly in the context of dysregulated signaling pathways and protein interactions that are characteristic of cancer cells.

Thesis goals – This study aimed to advance the current understanding of CAP generated through a plasma jet as a potential anti-cancer therapy by directly treating advanced three-dimensional (3D) models known as patient-derived tumor organoids (PDTOs). PDTOs are multicellular structures embedded into a 3D extracellular matrix that preserve the complex cellular heterogeneity within individual tumors and maintain genotype and phenotype, thereby providing a more accurate representation of the patient's specific disease characteristics (51, 52). To the best of current knowledge, this study represents one of the first to explore CAP application in PDTOs. Firstly, the response of PDTOs to CAP treatment was investigated to determine whether it aligns with findings reported in existing literature on the application of CAP in cancer treatment. Furthermore, the optimal CAP treatment conditions were identified to induce PTMs and ICD within PDTOs. By treating organoids derived from two highly aggressive and lethal cancers (HNSCC and PDAC), this study provided a comprehensive evaluation of CAP's effects across different patient populations and cancer types. Collectively, by combining advanced 3D organoid models, this research establishes a more translationally relevant platform for evaluating CAP-based therapies and further elucidates CAP's potential as an effective anti-cancer treatment that contributes to the development of more targeted and less toxic therapeutic strategies.

EXPERIMENTAL PROCEDURES

Organoid Culture – For this study, PDTOs derived from HNSCC and PDAC were cultured in OncoPro™ Basal Medium (Gibco™, Life Technologies, A55685-01) supplemented with various growth factors and supplements. For HNSCC PDTOs, the medium was supplemented with 100 units/mL penicillin/streptomycin (Gibco™, Life Technologies, 15140-122), 10 µM Y27 (Selleckchem, S1049), 2% B-27® supplement (Gibco™, Life Technologies, 17504-044), 2% OncoPro™ supplement (Gibco™, Life Technologies, A55686-01), 6.21% OncoPro™

Bovine Serum Albumin (BSA) (Gibco™, Life Technologies, A55686-01), and 10 ng/mL recombinant human fibroblast growth factor 10 (FGF-10) (Gibco™, Life Technologies, PHG0372). PDAC PDTOs were supplemented with the same components, with the addition of 10 nM Gastrin (Merck Life Sciences B.V., G9145). PDTOs were maintained at 37°C with 5% CO_2 in a humidified incubator, with medium changes twice a week. They were passaged at least once a week using TrypLE (Gibco™, Life Technologies, 12563-029) for dissociation, followed by centrifugation at 1500 rpm for 5 minutes at 4°C. Afterward, the cells were reseeded onto Cultrex (Bio-Techne, 3533-010-02), using the hanging droplet method and overlaid with the appropriate culture medium.

Plasma Source – Plasma treatment was performed using the neoplas kINPen IND-LAB. The device features a central rod-shaped electrode with a diameter of 1 mm, encased within a dielectric quartz capillary (outer diameter: 2 mm; inner diameter: 1.6 mm), and connected to a grounded ring electrode. A high-purity argon gas (99.999%, Air Liquide Belge N.V., P0021L50S2A001) was used as the feed gas at a flow rate of 2 standard liters per minute (slm). Plasma generation was driven by a sinusoidal voltage ranging from 1.0 to 1.1 MHz, with a maximum power output of 3.5 W. The voltage-induced gas discharge between the electrodes initiated the generation of reactive species inside the capillary, which were carried out with the gas flow as the active plasma effluent. The treatment was done with a fixed distance of 12 mm between the plasma nozzle and the surface of the target medium. The entire setup was automated and controlled using the WinPC-NC software to ensure consistent treatment conditions.

CAP Treatment – PDTOs (140 µL/well) were seeded into a Costar® clear, flat-bottom, ultra-low attachment 96-well plate (Corning Incorporated) that was coated with 7 µL of Cultrex (Bio-Techne, 3533-010-02), at a density of 1,500 PDTOs per well, one day prior to treatment, with 3-5 wells per condition. After overnight incubation at 37°C with 5% CO_2, the PDTOs were treated with the neoplas kINPen IND-LAB for various treatment times (30 sec, 1 min 30 sec, 2 min 30 sec, and 3 min 30 sec). In addition to the treatment groups, two controls were included: (1) a flow control, in which PDTOs were exposed to the gas flow only (no plasma) for 3 min 30 sec, and (2) a negative control, consisting of untreated PDTOs. For each assay, at least three independent experiments were performed.

Evaporation Experiment – To evaluate water evaporation during CAP treatment, the same protocol and treatment durations as previously described were applied. However, instead of organoid suspension, OncoPro™ Basal Medium (Gibco™, Life Technologies, A55685-01) (140 µL/well) was added to each well. After treatment, the remaining volume was collected with a pipette set to 140 µL. If air remained in the tip, the volume was gradually reduced until the medium could be fully aspirated without residual liquid or air. The evaporated volume was determined by subtracting the final aspirated volume from the initial 140 µL.

Growth Rate Assay – To determine the effect of CAP therapy on PDTO growth following the plasma treatment, 60 nM of IncuCyte Cytotox Reagent (ESSEN Biosciences, 4633) was added to each well. Subsequently, 30 minutes of incubation at 37°C and 5% CO_2, fluorescence images were captured using the Tecan Spark Cyto 600 live-cell imager. Imaging was performed using the brightfield and green fluorescence channels. The green channel corresponds to an excitation/emission range of 461-487 nm / 500-530 nm. Imaging was then continued every 12 hours until 72 hours post-treatment. Data was analyzed using Orbits software, and the growth rate was calculated by measuring changes in fluorescence intensity over time, combined with live-cell images of the PDTOs. Untreated PDTOs were used as negative controls, while the positive control consisted of PDTOs treated with 6 µM of Staurosporine, resulting in complete cell death.

RONS assessment – To quantify ROS and reactive nitrogen species (RNS), H_2O_2 and NO_2^- concentrations were quantified using the Fluorometric Hydrogen Peroxide Assay Kit (Sigma Aldrich, MAK165-1KT) and the Nitrate/Nitrite Fluorometric Assay Kit (Cayman Chemical, 780051), respectively, following the manufacturer's instructions. Initially, H_2O_2 and NO_2^- levels were assessed immediately after CAP treatment in the absence of PDTOs. Subsequently, to evaluate the uptake of these induced reactive species by PDTOs, H_2O_2 and NO_2^- levels were

measured in the presence of PDTOs post-CAP treatment. H_2O_2 levels were measured at two time points, right after the treatment and following a 2-hour incubation at 37°C with 5% CO_2 in a humidified incubator. NO_2^- level was measured after 2-hour and 4-hour incubation at 37°C with 5% CO_2. For NO_2^- quantification, all samples, except the controls, were diluted at a 1:50 ratio prior to measurement. In contrast, for H_2O_2 evaluation, only the 3-minute 30-second CAP treatment was diluted at a 1:50 ratio. Fluorescence was measured using the Tecan Spark Cyto 600 (Tecan, Switzerland) at excitation/emission wavelengths of 540/590 nm for H_2O_2 and 360/430 nm for NO_2^-. H_2O_2 and NO_2^- concentrations were then determined using the equations derived from their respective standard curves, which exhibited coefficients of determination (R^2) of 0.9976 and 0.8889, respectively.

$$H_2O_2 \text{concentration}(\mu M) = \frac{\text{Fluorescence of sample} - H_2O_2 \text{ standard curve intercept}}{H_2O_2 \text{ standard curve slope}}$$

$$NO_2^- \text{concentration}(\mu M) = \frac{\text{Fluorescence of sample} - NO_2^- \text{ standard curve intercept}}{NO_2^- \text{ standard curve slope}}$$

Total protein concentration measurement – To evaluate the impact of CAP treatment on total protein concentration, CAP treatment was conducted as previously described, using only 30 sec and 1 min 30 sec treatment, along with an untreated control. After 2-hour and 4-hour incubation at 37°C with 5% CO_2, total protein content was quantified using the Qubit™ Protein Broad Range (BR) Assay Kit (Thermo Fisher Scientific, A50668), according to the manufacturer's instructions. Fluorescence was measured using the Qubit 4 Fluorometer (Thermo Fisher Scientific, Q33238).

Analysis – All results were analyzed using one-way ANOVA with Prism 10 (GraphPad Software, USA). P value ≤0.05 was considered statistically significant. Data in all graphs are presented as the mean ± standard deviation (SD) except for the growth rate analysis, which is presented as the mean ± 95% confidence intervals (CI). The number of biological repeats is indicated in the figure legend. All statistical analyses and plots were done with GraphPad Prism 10 (GraphPad Software, USA).

RESULTS

Evaporation investigation post-CAP treatment – To examine whether CAP treatment evaporates water, the amount of medium was quantified before and after treatment across different CAP treatment durations (30 sec, 1 min 30 sec, 2 min 30 sec, 3 min 30 sec). While some evaporation was observed in the untreated control due to overnight incubation, the results demonstrated a CAP treatment duration-dependent increase in evaporated volume (Figure 3A). This additional loss became significantly pronounced at the highest CAP treatment durations (3 min 30 sec) compared to the untreated control ($p \leq 0.01$) (Figure 3A). This finding indicated that CAP contributes to water evaporation beyond incubation-related evaporation. Since this evaporation could influence downstream assay conditions, it was essential to quantify and compensate for the evaporated volume by adding water back into the wells in subsequent experiments.

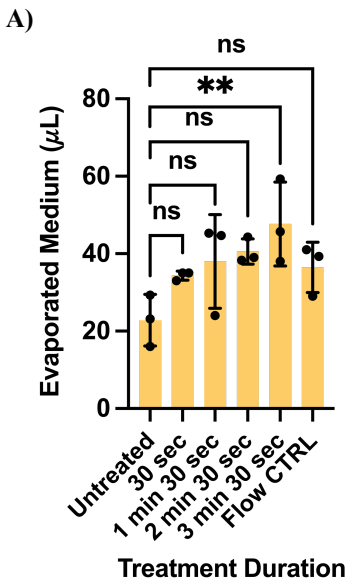

Figure. 3 – Evaluation of medium evaporation following CAP treatment. To assess CAP-induced water evaporation, the volume of culture medium was measured after CAP treatment at different treatment durations (30 sec, 1 min 30 sec, 2 min 30 sec, and 3 min 30 sec). Controls included untreated PDTOs (negative control), and flow control (Argon gas exposure without plasma for 3 min 30 sec). Results are presented as mean ± SD. Statistical analysis was performed using one-way ANOVA, and statistically significant is indicated as follows: ** $p \leq 0.01$, and *ns* = not significant. Number of biological replicates: $n = 3$

Determination of the CAP effect on PDTO growth – To investigate the impact of CAP treatment on tumor growth, the growth rate was monitored for 72 hours following treatment in PDTOs from four different candidates, two HNSCC patients, and two PDAC patients. PDTOs were treated with CAP for increasing treatment times (30 sec, 1 min 30 sec, 2 min 30 sec, 3 min 30 sec) to evaluate dose-dependent effects of CAP treatment. These were compared to three control conditions, including untreated PDTOs as the negative control, Staurosporine as a positive control (a highly potent apoptosis inducer due to its ability to inhibit a broad range of kinases), and a flow control group, in which PDTOs were exposed to Argon gas without plasma for 3 min 30 sec, to exclude any biological effects of the Argon flow from the CAP treatment. At the shortest treatment time (30 sec), a mild reduction in growth rate was observed in PDTOs from PDAC136, PDAC138, and HNSCC010 after almost 24 hours post-CAP treatment (Figure 4A, 4B, and 4D). Although this reduction was not statistically significant, it showed a detectable suppression of tumor growth compared to untreated PDTOs ($p=0.26$ and $p=0.78$, respectively). Notably, PDTOs from HNSC001 indicated no response to 30-sec CAP treatment, with a growth pattern comparable to untreated PDTOs (Figure 4C). Increasing the treatment time to 1 min 30 sec resulted in more notable growth suppression, specifically in PDTOs from PDAC136 and PDAC138, where a remarkable reduction in tumor growth was observed compared to untreated PDTOs ($p \leq 0.001$) (Figure 4A and 4B). Furthermore, this inhibitory effect remained stable over a 72-hour period. On the other hand, PDTOs from HNSCC 010 began to exhibit a gradual increase in growth after 24 hours following the initial decrease, and PDTOs from HNSCC001 showed a similar upward pattern starting at 60 hours post-treatment (Figure 4C and 4D). Although these PDTOs demonstrated a recovery in growth, the rate of increase remained modest and did not follow the sharp growth observed in the untreated controls. Likewise, 2 min 30 sec and 3 min 30 sec CAP treatment led to strong growth suppression across PDTOs from PDAC136 and PDAC138, with growth rates remaining low and closely resembling the effect seen with the positive control, where all PDTOs were eliminated by Staurosporin ($p \leq 0.0001$) (Figure 4A and 4B). In contrast, PDTOs from HNSCC001 and HNSCC010 showed fluctuating responses (Figure 4C and 4D). In HNSCC001, an initial decrease was observed during the first 12 hours post-treatment, followed by a temporary recovery that persisted until nearly 36 hours. Afterward, tumor growth reduced again and remained stable for the remaining 72-hour period (Figure 4C). A similar pattern was seen in PDTOs from HNSCC010, where a modest recovery in growth began in 24 hours post-CAP treatment and continued at a steady rate until the end of the 72-hour monitoring period (Figure 4D). However, this recovery was less pronounced following the 3 min 30 sec CAP treatment in PDTOs from HNSCC010 (Figure 4D). Although a slight recovery was observed at 24 hours following CAP treatment, the growth curve remained closely aligned with the Staurosporine curve, indicating sustained cytotoxic effects (Figure 4D). Besides these partial recoveries in HNSCC PDTOs, overall growth remained lower compared to the untreated controls following 1 min 30 sec or higher CAP treatments (Figure 4C and 4D). Importantly, PDTOs from PDAC displayed higher sensitivity to CAP treatment compared to PDTOs from HNSCC (Figure 4A-D). The growth of both PDTOs from PDAC136 and PDAC138 was almost completely arrested following treatments of 1 min 30 sec or higher exposures (Figure 4A and 4B). Moreover, unlike the partial recovery observed in HNSCC PDTOs, PDAC PDTOs did not exhibit any sign of growth enhancement across the different CAP treatment durations (Figure 4A-D). Another difference between PDAC and HNSCC PDTOs was their response to the flow control. While PDAC PDTOs exhibited a slight increase in growth, HNSCC PDTOs showed either a reduction or no change relative to the untreated control (Figure 4A-D). Together, these data demonstrate that CAP treatment inhibits the growth of cancer-derived organoids in a treatment duration-dependent manner and highlight the variability in treatment sensitivity between patients and cancer types.

Quantification of induced RONS following CAP treatment – To evaluate the level of reactive species generated by CAP, H_2O_2 and NO_2^- concentrations were measured immediately after CAP treatment at different treatment durations (30 sec, 1 min 30 sec, 2 min 30 sec, 3 min 30 sec) in the absence of PDTOs. These measurements were conducted to establish the baseline levels of RONS induced solely by CAP

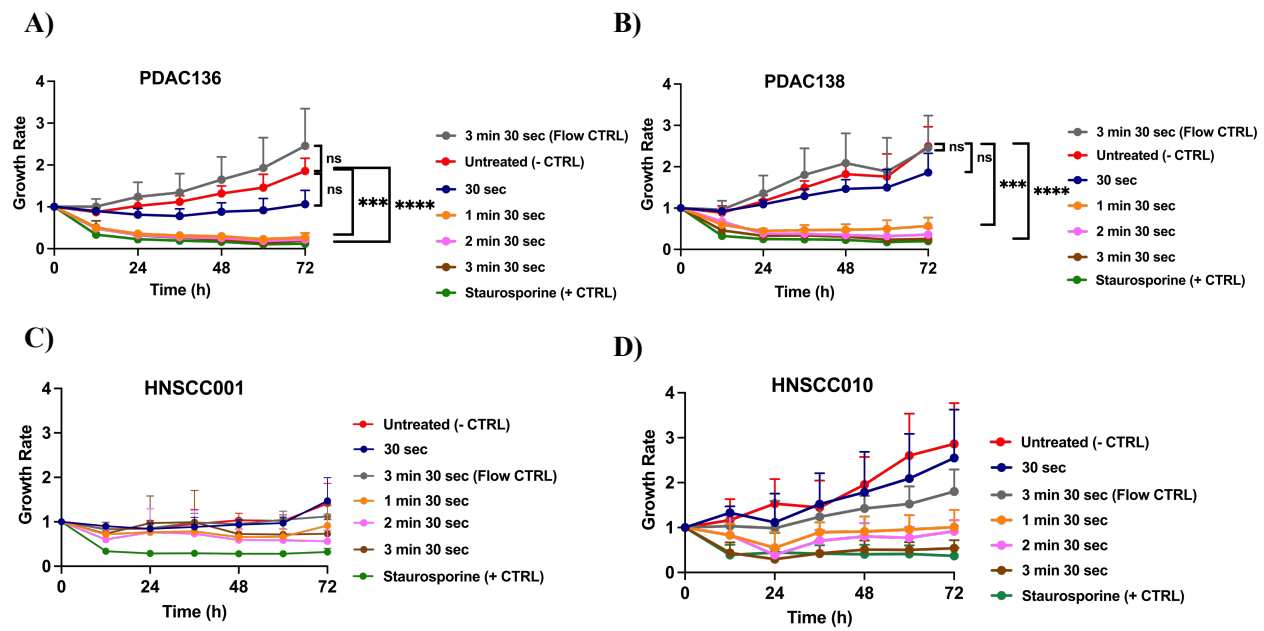

Figure. 4 – Growth rate of PDTOs following CAP treatment. Growth rates were monitored over 72 hours following CAP treatment at different exposure durations (30 sec, 1 min 30 sec, 2 min 30 sec, and 3 min 30 sec) of PDAC PDTOs (PDAC136, PDAC138) and HNSCC PDTOs (HNSCC001, HNSCC010). Live-cell imaging was performed throughout the monitoring period. Controls included untreated PDTOs (negative control), Staurosporine-treated PDTOs (positive control), and flow control (Argon gas exposure without plasma for 3 min 30 sec). The number of biological replicates varied by sample: PDAC136 (n = 4), and PDAC138 (n = 4), HNSCC001 (n = 2), and HNSCC010 (n = 1). Results are presented as mean ± 95% CI. Statistical analysis was performed using one-way ANOVA, and statistically significant is indicated as follows: $p \leq 0.001$ (***), $p \leq 0.0001$ (****); *ns* = not significant.

treatment. Since the medium used for culturing PDTOs from PDAC contained an additional supplement compared to the HNSCC medium, RONS levels were quantified separately in both media to account for possible differences in reactive species accumulation (Figure S1). NO_2^- levels remarkably increased in a CAP duration-dependent manner compared to controls in both PDAC and HNSCC medium (Figure 5A and Figure S1A). Although differences in NO_2^- concentrations between individual CAP treatment times were not statistically significant, a consistent gradual increase in NO_2^- levels were observed with longer treatment durations (Figure 5A and Figure S1A). In contrast, H_2O_2 concentrations did not show a statistically significant increase following CAP treatment, except at the longest treatment duration (3 min 30 sec), which resulted in a notable elevation in H_2O_2 concentration in both media (Figure 6A and Figure S1B). Interestingly, this sharp increase occurred despite only a one-minute difference from the 2 min 30 sec treatment, suggesting depletion of scavenging components present in the organoid culture medium. It is possible that after 2 min 30 sec, the medium's capacity to neutralize reactive species becomes saturated, leading to a more pronounced accumulation of H_2O_2. To further investigate this possibility, H_2O_2 levels were compared between Dulbecco's Modified Eagle Medium (DMEM) (used as cell culture medium) and advanced DMEM/F12 (used as organoid culture medium) following the same CAP treatment (Figure S2). The results indicated higher H_2O_2 concentrations in the cell culture medium, showing that the organoid culture medium likely contains scavengers that reduce the detectable levels of H_2O_2. To investigate whether PDTOs uptake or neutralize CAP-induced RONS, H_2O_2 and NO_2^- levels were measured at different time points following CAP treatment in the presence of PDTOs from PDAC136. Measurement of H_2O_2 concentrations immediately after CAP treatment revealed no detectable difference compared to organoid-free conditions, suggesting that PDTOs did not alter H_2O_2 levels at this early time point (Figure 6B). However, measurements conducted two hours post-CAP treatment showed that H_2O_2 was almost undetectable, indicating that PDTOs from

PDAC136 likely contributed to the uptake or degradation of H_2O_2 over time (Figure 6C). In contrast, NO_2^- concentrations, measured at two- and four-hour post-CAP treatment remained unchanged in the presence of PDTOs from PDAC136 (Figure 5B and 5C). Collectively, CAP exposure led to a treatment-dependent increase in NO_2^- and H_2O_2 levels. H_2O_2 levels declined over time in the presence of PDTOs, whereas NO_2^- levels remained stable. These findings characterize the pattern of RONS accumulation following CAP treatment and how it alters over time.

Total protein quantification after CAP treatment – To determine potential CAP-induced changes in protein content, total protein concentration was measured in PDTOs from PDAC136 at 2- and 4-hours following CAP treatment at 30 sec and 1 min 30 sec. Higher CAP treatment durations were excluded from this analysis, as extensive cell death observed in the growth rate assay prevented reliable protein quantification. No notable differences were observed in total protein concentrations between 30 sec and 1 min 30 sec CAP treatment groups, and protein levels remained comparable to protein concentration in untreated PDTOs from PDAC136 at both 2- and 4-hours following CAP treatment (Figure 7A and 7B). Similarly, no detectable alterations in protein levels were noticed between the 2- and 4-hour post-CAP treatment (Figure 7A and 7B).

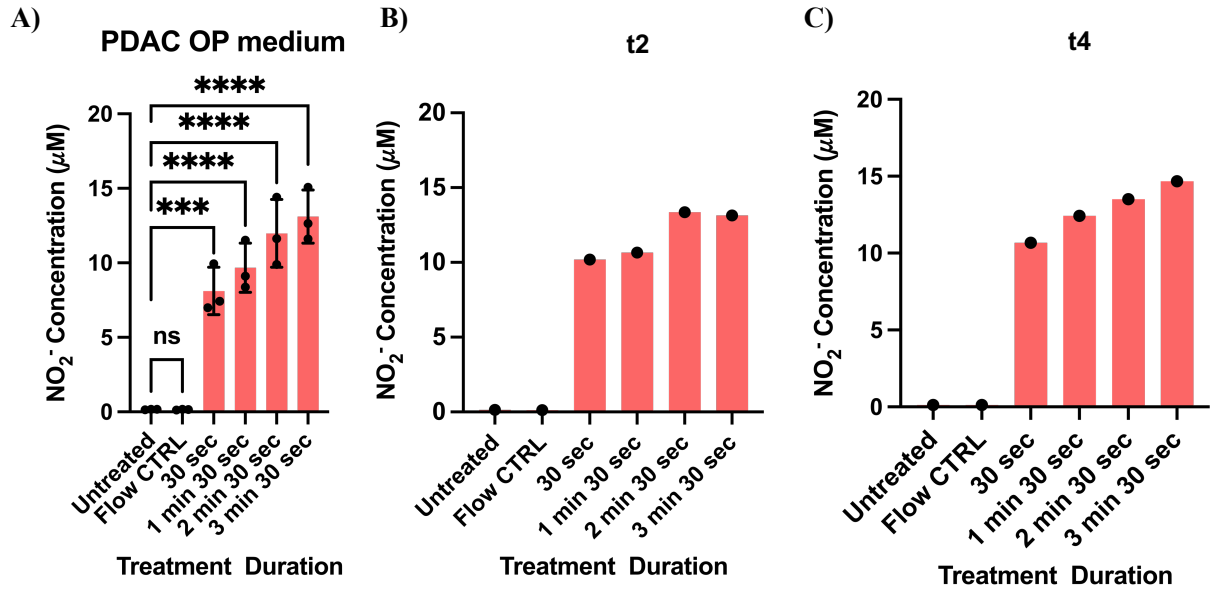

Figure. 5 – NO_2^- concentration in PDAC OP medium following CAP treatment in the absence and presence of PDTOs from PDAC136. NO_2^- levels were quantified using a fluorometric assay in PDAC organoid proliferation (OP) medium following CAP exposure at four treatment durations (30 sec, 1 min 30 sec, 2 min 30 sec, and 3 min 30 sec). Measurements were performed in the absence of PDTOs (**A**) and in the presence of PDTOs from PDAC136 2- and 4-hours post-treatment (**B, C**). Controls included untreated PDTOs (negative control) and flow control (Argon gas exposure without plasma for 3 min 30 sec). The number of biological replicates varied by sample: PDTO-free condition ($n = 3$) and PDTOs from PDAC136 conditions ($n = 1$). Results are presented as mean ± SD. Statistical analysis was performed using one-way ANOVA, and statistically significant is indicated as follows: $p \leq 0.001$ (***), $p \leq 0.0001$ (****); *ns* = not significant.

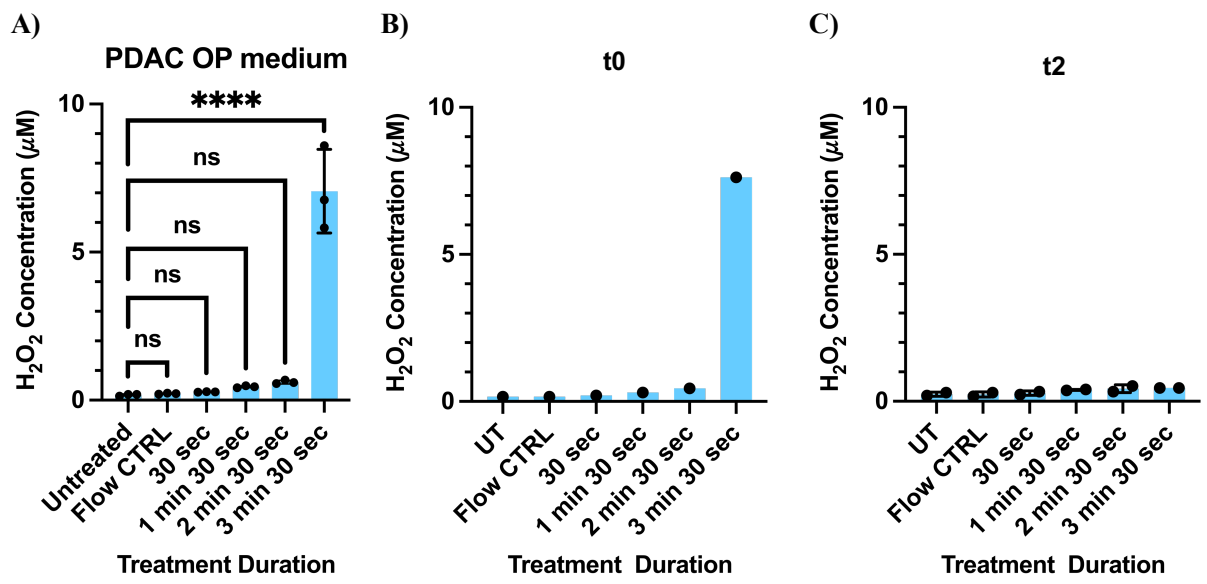

Figure 6. H_2O_2 concentration in PDAC OP medium following CAP treatment in the absence and presence of PDTOs from PDAC136. H_2O_2 levels were quantified using a fluorometric assay in PDAC OP medium following CAP exposure at four treatment durations (30 sec, 1 min 30 sec, 2 min 30 sec, and 3 min 30 sec). Measurements were performed in the absence of PDTOs (**A**) and in the presence of PDTOs from PDAC136 immediately after treatment and 2 hours post-CAP treatment (**B**, **C**). Controls included untreated PDTOs (negative control) and flow control (Argon gas exposure without plasma for 3 min 30 sec). The number of biological replicates varied by sample: PDTO-free condition ($n = 3$) and PDTOs from PDAC136 condition: $n = 1$ (immediately after treatment) and $n = 2$ (2 hours post-treatment). Results are presented as mean ± SD. Statistical analysis was performed using one-way ANOVA, and statistically significant is indicated as follows: $p \leq 0.0001$ (****); *ns* = not significant.

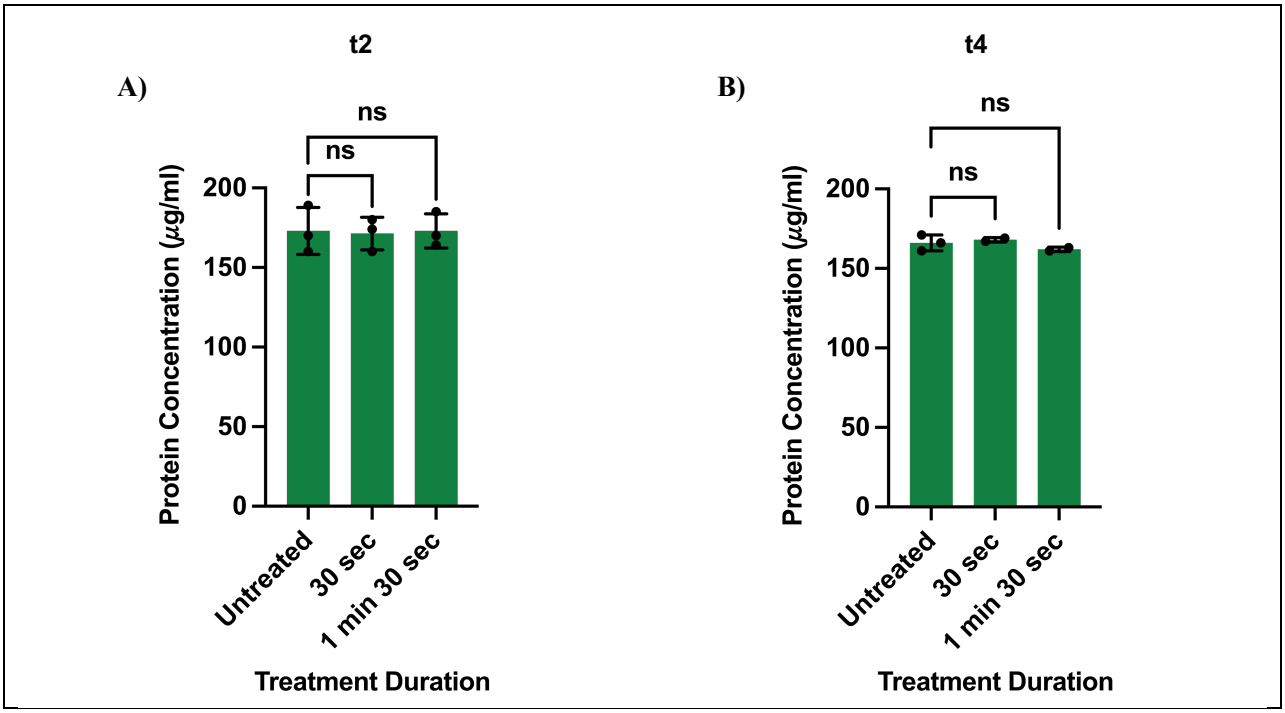

Figure 7. Total protein concentration in PDTOs from PDAC136 following CAP treatment. PDTOs from PDAC136 were treated with CAP for 30 seconds or 1 min 30 sec, and total protein concentration was measured at 2- and 4-hours post-treatment using Qubit™ Protein BR Assay. Results are presented as mean ± SD. Statistical analysis was conducted using one-way ANOVA. *ns* = not significant. Number of biological replicates: $n = 3$

DISCUSSION & CONCLUSION

CAP is a promising emerging approach in cancer therapy (53). The growing interest in CAP as a novel cancer treatment is largely attributed to its observed selectivity towards targeting cancer cells. A primary mechanism underlying CAP's anticancer activity is the elevation of ROS levels (54). Since cancer cells typically exhibit higher levels of endogenous RONS compared to normal cells, their antioxidant responses are overwhelmed easily (55). Hence, they are less efficient at repairing CAP-induced oxidative damage, making them more sensitive to CAP treatment (54). Several studies have reported CAP-induced cytotoxic effects across various cancer cell types, including brain, lung, blood, cervical, and melanoma, among others (56). However, the majority of this research has been conducted using 2D cell cultures and mouse models, which have inherent limitations and fail to accurately represent the complexity of human tumor biology. To address these limitations, this study investigated CAP effects on two aggressive cancer types using PDTOs, a more physiologically relevant and translationally meaningful model. In this study, we aimed to investigate how PDTOs respond to CAP treatment and to determine whether their responses align with the CAP sensitivity previously reported in conventional 2D cancer cell lines. Our findings demonstrated that CAP exerted dose-dependent cytotoxic effects on PDTO cultures, aligning with previous reports using 2D cancer cell culture (57). Notably, a differential response was observed between the two PDTO models. PDTOs from PDAC were remarkably sensitive to CAP treatment compared to HNSCC PDTOs. CAP treatment almost completely arrested the growth of PDAC PDTOs, with no recovery observed over the 72-hour post-treatment period. In contrast, HNSCC PDTOs displayed an initial growth suppression after CAP treatment that was followed by partial regrowth during the rest of the monitoring period, except for HNSCC010 at the highest CAP treatment, which showed almost complete growth inhibition. This variation suggests that CAP treatment parameters used in this study, like exposure durations, applied voltage, and gas flow rate, were sufficient to induce sustained growth suppression in PDAC PDTOs but were less effective in HNSCC PDTOs. Therefore, optimizing these physical parameters to generate a more reactive plasma, for instance by increasing gas flow rate, extending the treatment times, or applying multiple treatments, may be necessary to achieve a comparable cytotoxic effect in PDTOs from HNSCC. Additionally, the evaporation evaluation following CAP treatment enabled minimization of the potential impact on PDTO growth, by restoring the evaporated water in the PDTO culture after CAP treatment. Hence, the observed cytotoxic effects were specifically attributed to CAP treatment. Furthermore, the observed difference in CAP sensitivity between PDAC- and HNSCC-PDTOs likely reflects intrinsic biological differences between these cancer types. HNSCC may possess more robust antioxidant responses that help neutralize CAP-induced oxidative damage. For instance, Stacy *et al.* have demonstrated that HNSCC overexpress nuclear factor erythroid 2-related factor 2 (NRF2), which plays a pivotal role in controlling the expression of genes that protect cells against oxidative stress and facilitate the detoxification of reactive species (58, 59). Additionally, Namani *et al.* have reported Kelch-like-ECH-associated protein 1, which negatively regulates NRF2 expression through proteasomal degradation, loses its function in HNSCC patients (59). This dysregulation in the NFR2/KEAP1 axis results in higher antioxidant capacity and resistance to oxidative stress in HNSCC.

To date, many studies have identified RONS as key mediators of CAP cytotoxic effects. Therefore, we quantified RONS induction following CAP treatment in PDTO culture medium. Our findings indicate that H_2O_2 and NO_2^- levels increase in a duration-dependent manner following CAP treatment to organoid culture medium. However, this increase was not statistically significant for H_2O_2 concentration, except for the highest CAP treatment duration (3 min 30 sec). Organoid growth needs a complex medium including several supplements that provide antioxidants and radical scavengers. For instance, B27 supplement contains various enzymatic and nonenzymatic antioxidants such as

catalase and superoxide dismutase (60). Additionally, bovine serum albumin in organoid culture medium can directly or indirectly neutralize free radicals and ROS (61). This suggests that a portion of H_2O_2 may have been neutralized by these components, resulting in lower detectable H_2O_2 in shorter CAP treatment durations. Moreover, since the culture media for HNSCC- and PDAC-PDTOs differ slightly in composition, H_2O_2 and NO_2^- concentrations were quantified separately to assess potential differences in measurable induced reactive species following CAP treatment. The results indicated that H_2O_2 and NO_2^- concentrations were comparable between these two types of media following CAP treatment, suggesting this difference had no detectable impact on measurable concentrations of induced reactive species post-CAP treatment. Generally, our results were consistent with previous studies, indicating that H_2O_2 and NO_2^- concentrations increase in a CAP treatment time-dependent manner (62-64). However, the concentrations of induced H_2O_2 and NO_2^- in organoid culture medium were relatively lower compared to those reported in studies using other media, such as PBS, DI water, or DMEM/10% fetal bovine serum, under almost similar flow rates and treatment durations (62-64). This difference can likely be attributed to the presence of scavenging components in organoid culture medium, which may have quenched part of the reactive species generated during CAP treatment. Next, we examined the uptake of these induced RONS following CAP treatment by PDTOs. Although PDAC PDTOs absorbed almost all induced H_2O_2 two hours post-treatment, they did not significantly alter NO_2^- levels at both 2- and 4-hours following CAP treatment. One possible explanation is that the short-lived reactive nitrogen species generated by CAP, like nitric oxide and peroxynitrite are gradually converted into NO_2^- during the post-treatment incubation period (65, 66). This ongoing conversion into NO_2^- likely contributed to a gradual increase in NO_2^- level over time, potentially masking any reduction thanks to biological uptake by PDTOs. Consequently, the overall NO_2^- concentration remained relatively constant, as the continuous formation of NO_2^- may have compensated for any internalization or metabolization in NO_2^- levels by PDTOs from PDAC.

Although our findings demonstrated the promising potential of CAP in reducing the growth of HNSCC- and PDAC-PDTOs, further investigations are needed to strengthen and validate these results. In terms of HNSCC PDTOs, two experimental repeats were conducted for the growth rate of HNSCC001 and only one repeat for HNSCC010. Additional biological replicates are needed for these HNSCC PDTOs to strengthen the reliability of these findings. Even though four repeats were performed for each PDAC PDTO, the study evaluated PDTOs from only two candidates per cancer type. Therefore, to better capture biological variability across different tumors and individuals and enhance the reliability of our findings, further validation with a larger cohort of organoids derived from diverse patient samples is required. However, the well-recognized limitations of PDTO models should not be underestimated. The establishment of PDTOs is costly, time-consuming, and technically challenging, with reported success rates varying widely across samples and cancer types, ranging from 15% to 90% (67, 68). Likewise, in our laboratory (CORE), the initial success rate for generating PDTOs from HNSCC and PDACC samples is almost 80-90%. However, this success rate for establishing long-term surviving PDTOs from these cancer types dramatically reduced to around 20%. Moreover, Velasco *et al.* have shown that the reproducibility of PDTOs can vary even when following the same conditions (69). Besides all their challenges, PDTOs still provide a more biologically relevant in vitro platform compared to conventional models like 2D cell lines.

As a next step, following our findings that CAP can induce cytotoxicity in cancer-derived organoids and the induced RONS may be internalized by them, we aim to further investigate whether CAP can also activate ICD in PDTOs by measuring various ICD markers such as CRT, HMGB1, and ATP. Demonstrating the presence of these ICD markers for CAP-treated PDAC and HNSCC PDTOs would indicate that CAP not only eliminates cancer cells but also transforms them into stimulants for the immune system and facilitates long-term tumor control (70). Furthermore, another avenue for future research involves delving into induced modifications at the protein level following CAP treatment. Interestingly, our primary investigation indicated that CAP treatment did not significantly alter the total protein concentrations in PDTOs, as the overall protein level remained relatively comparable to untreated PDTOs. This suggests that CAP's effect on protein profile may be more qualitative than quantitative. To examine this

hypothesis, we plan to employ proteomic analyses to identify alterations in protein expression and PTMs following CAP treatment in our PDTO models.

To conclude, this study, by demonstrating the suppression in growth of cancer-derived organoids, has revealed the potential and challenges of CAP application on PDTOs. The differential sensitivity between cancer types and the interactions of CAP-induced reactive species with components of organoid culture medium have provided valuable insights for optimizing CAP treatment parameters. By addressing these challenges and pursuing the proposed future study, including ICD activation and PTMs at the protein level following CAP treatment, we can deepen our understanding of CAP mechanisms. This knowledge will not only strengthen the experimental rigor of CAP studies in organoid models but also guide the translation of CAP into clinical settings. Finally, these efforts aim to advance the understanding of CAP as an innovative anticancer approach and contribute to the development of more effective therapies for patients with aggressive cancers like PDAC and HNSCC.

REFERENCES

1. Panegyres K. The story of how cancer got its name. Cancer. 2024;130(20):3401-3.
2. Sarkar S, Horn G, Moulton K, Oza A, Byler S, Kokolus S, et al. Cancer development, progression, and therapy: an epigenetic overview. Int J Mol Sci. 2013;14(10):21087-113.
3. Kumar G, Virmani T, Sharma A, Pathak K. Codelivery of Phytochemicals with Conventional Anticancer Drugs in Form of Nanocarriers. Pharmaceutics. 2023;15(3).
4. Sung H, Ferlay J, Siegel RL, Laversanne M, Soerjomataram I, Jemal A, et al. Global Cancer Statistics 2020: GLOBOCAN Estimates of Incidence and Mortality Worldwide for 36 Cancers in 185 Countries. CA Cancer J Clin. 2021;71(3):209-49.
5. Manzari-Tavakoli A, Babajani A, Tavakoli MM, Safaeinejad F, Jafari A. Integrating natural compounds and nanoparticle-based drug delivery systems: A novel strategy for enhanced efficacy and selectivity in cancer therapy. Cancer Med. 2024;13(5):e7010.
6. Aseafan Mohamed, Alfakeeh Ali H., Tashkandi Emad, Mahrous Mervat, Alghamdi Mohammed, Alshamsan Bader, et al. Real-world clinical outcome of unresectable locally advanced & de-novo metastatic pancreatic ductal adenocarcinoma: a multicentre retrospective study. Springer Nature Link. 2025;25.
7. Fanijavadi S, Thomassen M, Jensen LH. Targeting Triple NK Cell Suppression Mechanisms: A Comprehensive Review of Biomarkers in Pancreatic Cancer Therapy. Int J Mol Sci. 2025;26(2).
8. Du J, Gu J, Li J. Mechanisms of drug resistance of pancreatic ductal adenocarcinoma at different levels. Biosci Rep. 2020;40(7).
9. Pingping Z, Nan C, Yong T. Phytochemicals and their Nanoformulations for Overcoming Drug Resistance in Head and Neck Squamous Cell Carcinoma. Pharm Res. 2025;42(3):429-49.
10. Li HS, Tang R, Shi HS, Qin ZJ, Zhang XY, Sun YF, et al. Ultra-high dose rate radiotherapy overcomes radioresistance in head and neck squamous cell carcinoma. Signal Transduct Target Ther. 2025;10(1):82.
11. Khera N, Rajkumar AS, Abdulkader MAK, Liu Z, Ma H, Waseem A, et al. Identification of multidrug chemoresistant genes in head and neck squamous cell carcinoma cells. Mol Cancer. 2023;22(1):146.
12. Marquard FE, Jucker M. PI3K/AKT/mTOR signaling as a molecular target in head and neck cancer. Biochem Pharmacol. 2020;172:113729.
13. Robatel S, Schenk M. Current Limitations and Novel Perspectives in Pancreatic Cancer Treatment. Cancers (Basel). 2022;14(4).
14. Kozakiewicz P, Grzybowska-Szatkowska L. Application of molecular targeted therapies in the treatment of head and neck squamous cell carcinoma. Oncol Lett. 2018;15(5):7497-505.
15. Siqueira JM, Heguedusch D, Rodini CO, Nunes FD, Rodrigues M. Mechanisms involved in cancer stem cell resistance in head and neck squamous cell carcinoma. Cancer Drug Resist. 2023;6(1):116-37.
16. Zhang Z, Song B, Wei H, Liu Y, Zhang W, Yang Y, et al. NDRG1 overcomes resistance to immunotherapy of pancreatic ductal adenocarcinoma through inhibiting ATG9A-

dependent degradation of MHC-1. Drug Resist Updat. 2024;73:101040.
17. Barham William T., Stagg Marshall Patrick, Mualla Rula, DiLeo Michael, Sagar K. Recurrent and Metastatic Head and Neck Cancer: Mechanisms of Treatment Failure, Treatment Paradigms, and New Horizons. Cancers 2025.
18. Tan E, El-Rayes B. Pancreatic Cancer and Immunotherapy: Resistance Mechanisms and Proposed Solutions. J Gastrointest Cancer. 2019;50(1):1-8.
19. Liu X, Harbison RA, Varvares MA, Puram SV, Peng G. Immunotherapeutic strategies in head and neck cancer: challenges and opportunities. J Clin Invest. 2025;135(8).
20. Guo Z, Li K, Ren X, Wang X, Yang D, Ma S, et al. The role of the tumor microenvironment in HNSCC resistance and targeted therapy. Front Immunol. 2025;16:1554835.
21. Ratovitski Edward A., Cheng Xiaoqian, Yan Dayun, Sherman Jonathan H., Canady Jerome, Trink Barry, et al. Anti-Cancer Therapies of 21st Century: Novel Approach to Treat Human Cancers Using Cold Atmospheric Plasma. WILEY. 2014.
22. Wang Y, Mang X, Li D, Wang Z, Chen Y, Cai Z, et al. Cold atmospheric plasma sensitizes head and neck cancer to chemotherapy and immune checkpoint blockade therapy. Redox Biol. 2024;69:102991.
23. Verloy R, Privat-Maldonado A, Smits E, Bogaerts A. Cold Atmospheric Plasma Treatment for Pancreatic Cancer-The Importance of Pancreatic Stellate Cells. Cancers (Basel). 2020;12(10).
24. Brany D, Dvorska D, Strnadel J, Matakova T, Halasova E, Skovierova H. Effect of Cold Atmospheric Plasma on Epigenetic Changes, DNA Damage, and Possibilities for Its Use in Synergistic Cancer Therapy. Int J Mol Sci. 2021;22(22).
25. Fu Danni, Lin Shiyao, Xu Qingnan, Cao Fei, Khan Israr, Xu Shu, et al. Cold atmospheric plasma as novel 'drug' for cancer therapy. Authorea. 2025.
26. B. GD. Reactive Species from Cold Atmospheric Plasma: Implications for Cancer Therapy. WILEY. 2014.
27. Sklias K, Santos Sousa J, Girard PM. Role of Short- and Long-Lived Reactive Species on the Selectivity and Anti-Cancer Action of Plasma Treatment In Vitro. Cancers (Basel). 2021;13(4).
28. Yan Dayun, Cui Haitao, Zhu Wei, Talbot Annie, Zhang Lijie Grace, Sherman Jonathan H., et al. The Strong Cell-based HydrogenPeroxide Generation Triggered by Cold Atmospheric Plasma. Scientific Reports. 20217.
29. Chupradit S, Widjaja G, Radhi Majeed B, Kuznetsova M, Ansari MJ, Suksatan W, et al. Recent advances in cold atmospheric plasma (CAP) for breast cancer therapy. Cell Biol Int. 2023;47(2):327-40.
30. Woedtke Thomas von, Bekeschus Sander, Weltmann Klaus-Dieter, Kristian W. Plasma-Treated Liquids for Medicine: A Narrative Review on State and Perspectives. WILEY. 2024.
31. Yan Dayun, Malyavko Alisa, Wang Qihui, Lin Li, Sherman Jonathan H., Michael K. Cold Atmospheric Plasma Cancer Treatment, a Critical Review. Applied Sciences. 2021.
32. Seong Min-Jeong, Park Kyu-Ri, Kim S. J., Joh Hea-Min, Moon Hanul, Chung T. H. Characterization and bacterial inactivation application of multiple pin-to-plate electrode-based DBD plasma driven by nanosecond-pulsed high voltage. Physics of Plasma. 2025.
33. Holanda AGA, Francelino LEC, Moura CEB, Alves Junior C, Matera JM, Queiroz GF. Cold Atmospheric Plasma in Oncology: A Review and Perspectives on Its Application in Veterinary Oncology. Animals (Basel). 2025;15(7).
34. Stańczyk Beata, Marek W. The Promising Potential of Cold Atmospheric Plasma Therapies. Plasma 2024.
35. Biscop E, Baroen J, De Backer J, Vanden Berghe W, Smits E, Bogaerts A, et al. Characterization of regulated cancer cell death pathways induced by the different modalities of non-thermal plasma treatment. Cell Death Discov. 2024;10(1):416.
36. Jeong Eun Ji, Park Hyun Min , Lee Dong Jae, Lee Jun, Cho Jun Yeong , Seo Kyung Deok, et al. Clinical application of cold atmospheric-pressure plasma: mechanisms and irradiation conditions. IOP Science. 2024.
37. Brany D, Dvorska D, Halasova E, Skovierova H. Cold Atmospheric Plasma: A Powerful Tool for Modern Medicine. Int J Mol Sci. 2020;21(8).
38. Szlasa W, Zendran I, Zalesinska A, Tarek M, Kulbacka J. Lipid composition of the cancer cell membrane. J Bioenerg Biomembr. 2020;52(5):321-42.

39. Almeida-Ferreira C, Rodrigues F, Marto CM, Botelho MF, Laranjo M. Cold atmospheric plasma for breast cancer treatment: what next? Med Gas Res. 2025;15(1):110-1.
40. Zhang M, Zhou G, Xu Y, Wei B, Liu Q, Zhang G, et al. Immunogenic cell death signature predicts survival and reveals the role of VEGFA + Mast cells in lung adenocarcinoma. Sci Rep. 2025;15(1):7213.
41. Yoon Y, Ku B, Lee K, Jung YJ, Baek SJ. Cold Atmospheric Plasma Induces HMGB1 Expression in Cancer Cells. Anticancer Res. 2019;39(5):2405-13.
42. Heirman Pepijn, Verswyvel Hanne, Bauwens Mauranne, Yusupov Maksudbek, Waele Jorrit De, Lin Abraham, et al. Effect of plasma-induced oxidation on NK cell immune checkpoint ligands: A computational-experimental approach. ELSEVIER. 2024.
43. Chai Zhao-Nan, Wang Xu-Cheng, Yusupov Maksudbek, Yuan-Tao Z. Unveiling the interaction mechanisms of cold atmospheric plasma and amino acids by machine learning. PLASMA PROCESSES AND POLYMERS. 2024;21(7).
44. Zivanic M, Espona-Noguera A, Lin A, Canal C. Current State of Cold Atmospheric Plasma and Cancer-Immunity Cycle: Therapeutic Relevance and Overcoming Clinical Limitations Using Hydrogels. Adv Sci (Weinh). 2023;10(8):e2205803.
45. Yusupov M, Privat-Maldonado A, Cordeiro RM, Verswyvel H, Shaw P, Razzokov J, et al. Oxidative damage to hyaluronan-CD44 interactions as an underlying mechanism of action of oxidative stress-inducing cancer therapy. Redox Biol. 2021;43:101968.
46. Lin A, Razzokov J, Verswyvel H, Privat-Maldonado A, De Backer J, Yusupov M, et al. Oxidation of Innate Immune Checkpoint CD47 on Cancer Cells with Non-Thermal Plasma. Cancers (Basel). 2021;13(3).
47. Foo MA, You M, Chan SL, Sethi G, Bonney GK, Yong WP, et al. Clinical translation of patient-derived tumour organoids- bottlenecks and strategies. Biomark Res. 2022;10(1):10.
48. Drost J, Clevers H. Organoids in cancer research. Nat Rev Cancer. 2018;18(7):407-18.
49. Nagle PW, Plukker JTM, Muijs CT, van Luijk P, Coppes RP. Patient-derived tumor organoids for prediction of cancer treatment response. Semin Cancer Biol. 2018;53:258-64.
50. Schlegel Jürgen, Köritzer Julia, Boxhammer Veronika. Plasma in cancer treatment. ELSEVIER. 2013.
51. Abbasian MH, Sobhani N, Sisakht MM, D'Angelo A, Sirico M, Roudi R. Patient-Derived Organoids: A Game-Changer in Personalized Cancer Medicine. Stem Cell Rev Rep. 2025;21(1):211-25.
52. Zhao Z, Chen X, Dowbaj AM, Sljukic A, Bratlie K, Lin L, et al. Organoids. Nat Rev Methods Primers. 2022;2.
53. Saadati Fariba, Jahanbakhshi Fahimeh, Mahdikia Hamed, Abbasvandi Fereshteh, Ghomi Hamid, Yazdani Nasrin, et al. Cold Physical Plasma Toxicity in Breast and Oral Squamous Carcinoma In Vitro and in Patient-Derived Cancer Tissue Ex Vivo. Applied Sciences. 2023.
54. Pavlovic O, Lazarevic M, Jakovljevic A, Skoro N, Puac N, Mojsilovic S, et al. Antitumor Potential of Different Treatment Approaches Using Cold Atmospheric Pressure Plasma on Oral Squamous Cell Carcinoma Models: In Vitro Study. Biomedicines. 2025;13(2).
55. Privat-Maldonado A, Verloy R, Cardenas Delahoz E, Lin A, Vanlanduit S, Smits E, et al. Cold Atmospheric Plasma Does Not Affect Stellate Cells Phenotype in Pancreatic Cancer Tissue in Ovo. Int J Mol Sci. 2022;23(4).
56. Dubuc A, Monsarrat P, Virard F, Merbahi N, Sarrette JP, Laurencin-Dalicieux S, et al. Use of cold-atmospheric plasma in oncology: a concise systematic review. Ther Adv Med Oncol. 2018;10:1758835918786475.
57. Yan D, Talbot A, Nourmohammadi N, Cheng X, Canady J, Sherman J, et al. Principles of using Cold Atmospheric Plasma Stimulated Media for Cancer Treatment. Sci Rep. 2015;5:18339.
58. Stacy DR, Ely K, Massion PP, Yarbrough WG, Hallahan DE, Sekhar KR, et al. Increased expression of nuclear factor E2 p45-related factor 2 (NRF2) in head and neck squamous cell carcinomas. Head Neck. 2006;28(9):813-8.
59. Namani A, Matiur Rahaman M, Chen M, Tang X. Gene-expression signature regulated by the KEAP1-NRF2-CUL3 axis is associated with a poor prognosis in head and neck squamous cell cancer. BMC Cancer. 2018;18(1):46.
60. Roth S, Zhang S, Chiu J, Wirth EK, Schweizer U. Development of a serum-free supplement for primary neuron culture reveals the interplay of selenium and vitamin E in neuronal

survival. J Trace Elem Med Biol. 2010;24(2):130-7.
61. Watanabe K, Kinoshita H, Okamoto T, Sugiura K, Kawashima S, Kimura T. Antioxidant Properties of Albumin and Diseases Related to Obstetrics and Gynecology. Antioxidants (Basel). 2025;14(1).
62. Jo A, Joh HM, Bae JH, Kim SJ, Chung JW, Chung TH. Plasma-Activated Media Produced by a Microwave-Excited Atmospheric Pressure Plasma Jet Is Effective against Cisplatin-Resistant Human Bladder Cancer Cells In Vitro. Int J Mol Sci. 2024;25(2).
63. Feibel D, Golda J, Held J, Awakowicz P, Schulz-von der Gathen V, Suschek CV, et al. Gas Flow-Dependent Modification of Plasma Chemistry in muAPP Jet-Generated Cold Atmospheric Plasma and Its Impact on Human Skin Fibroblasts. Biomedicines. 2023;11(5).
64. Chen CY, Chou CH, Cheng YC. The Genetic Expression Difference of A2058 Cells Treated by Plasma Direct Exposure and Plasma-Treated Medium and the Appropriate Treatment Strategy. Biomedicines. 2025;13(1).
65. Sun Jie, Zhang Xueji, Broderick Mark, Harry F. Measurement of Nitric Oxide Production in Biological Systems by Using Griess Reaction Assay. Sensor. 2003.
66. Lindemann C, Lupilova N, Muller A, Warscheid B, Meyer HE, Kuhlmann K, et al. Redox proteomics uncovers peroxynitrite-sensitive proteins that help Escherichia coli to overcome nitrosative stress. J Biol Chem. 2013;288(27):19698-714.
67. Hou X, Du C, Lu L, Yuan S, Zhan M, You P, et al. Opportunities and challenges of patient-derived models in cancer research: patient-derived xenografts, patient-derived organoid and patient-derived cells. World J Surg Oncol. 2022;20(1):37.
68. Qu J, Kalyani FS, Liu L, Cheng T, Chen L. Tumor organoids: synergistic applications, current challenges, and future prospects in cancer therapy. Cancer Commun (Lond). 2021;41(12):1331-53.
69. Velasco S, Kedaigle AJ, Simmons SK, Nash A, Rocha M, Quadrato G, et al. Individual brain organoids reproducibly form cell diversity of the human cerebral cortex. Nature. 2019;570(7762):523-7.
70. Fucikova J, Kepp O, Kasikova L, Petroni G, Yamazaki T, Liu P, et al. Detection of immunogenic cell death and its relevance for cancer therapy. Cell Death Dis. 2020;11(11):1013.
GenAI has been utilized to enhance academic English and provide support with grammar.

Acknowledgements – I would like to express my sincere gratitude to my supervisors, Dr. Angela Privat Maldonado and Jana Baroen, for their continuous guidance, valuable feedback, and encouragement throughout this project.
This work was supported by funding from the Flemish Institute for Technological Research (VITO) and the Methusalem grant of Prof. Dr. A. Bogaerts. I gratefully acknowledge the University Hospital of Antwerp (UZA) and the patients for providing the tumor samples essential to this study. I would also like to thank the Tumoroid Screening Lab at CORE, the Tumor Organoid Biobank, and the High-throughput Screening Facility (DrugVision.ai) at the University of Antwerp for providing fully optimised protocols for patient-derived organoid generation, drug screening, and image analysis. Special thanks to Orbits for the use of their software in the data analysis pipeline.

Author contributions – Jana Baroen conceived and designed the research. Jana Baroen and Sara Esbati performed the experiments. Sara Esbati conducted the data analysis and wrote the thesis. Dr. Angela Privat Maldonado and Jana Baroen reviewed and edited the final text. Dr. Angela Privat Maldonado and Jana Baroen supervised the project.

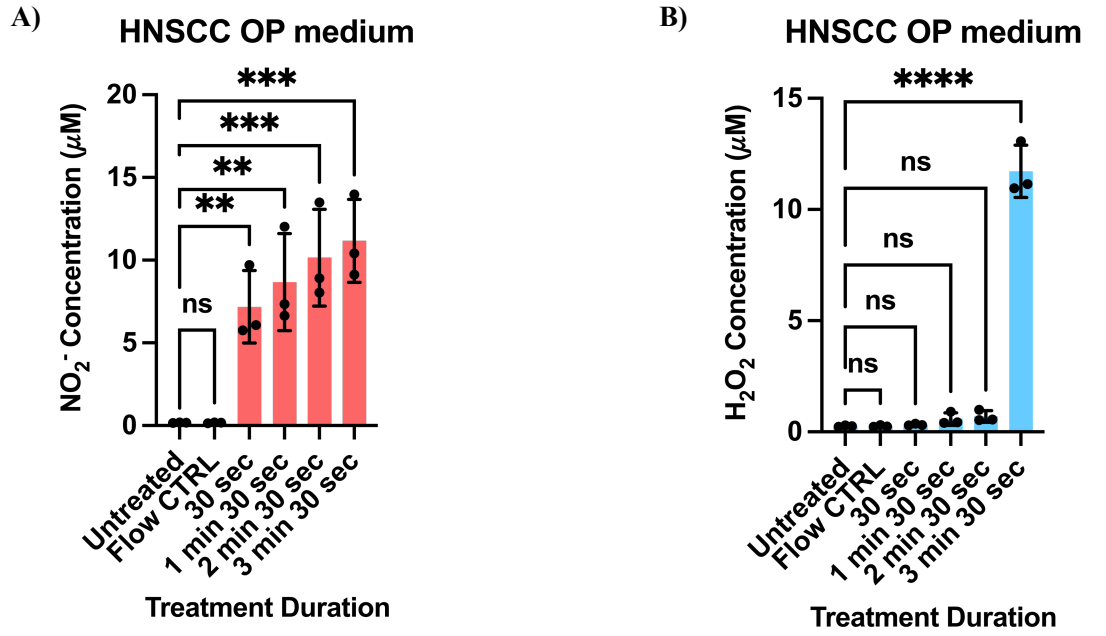

Figure S1. RONS quantification in HNSCC OP medium following CAP treatment. H_2O_2 and NO_2^- concentrations were measured using fluorometric assays in HNSCC OP medium following CAP treatment at four treatment durations (30 sec, 1 min 30 sec, 2 min 30 sec, and 3 min 30 sec). Measurements were performed in organoid-free conditions to assess baseline RONS induction. Data are presented as mean ± SD. Statistical analysis was conducted using one-way ANOVA. Statistical significance is indicated as follows: $^{**}p < 0.01$, $^{***}p < 0.001$, and $^{****}p < 0.0001$; *ns* = not significant. Number of biological replicates: $n = 3$ for both H_2O_2 and NO_2^- measurements.

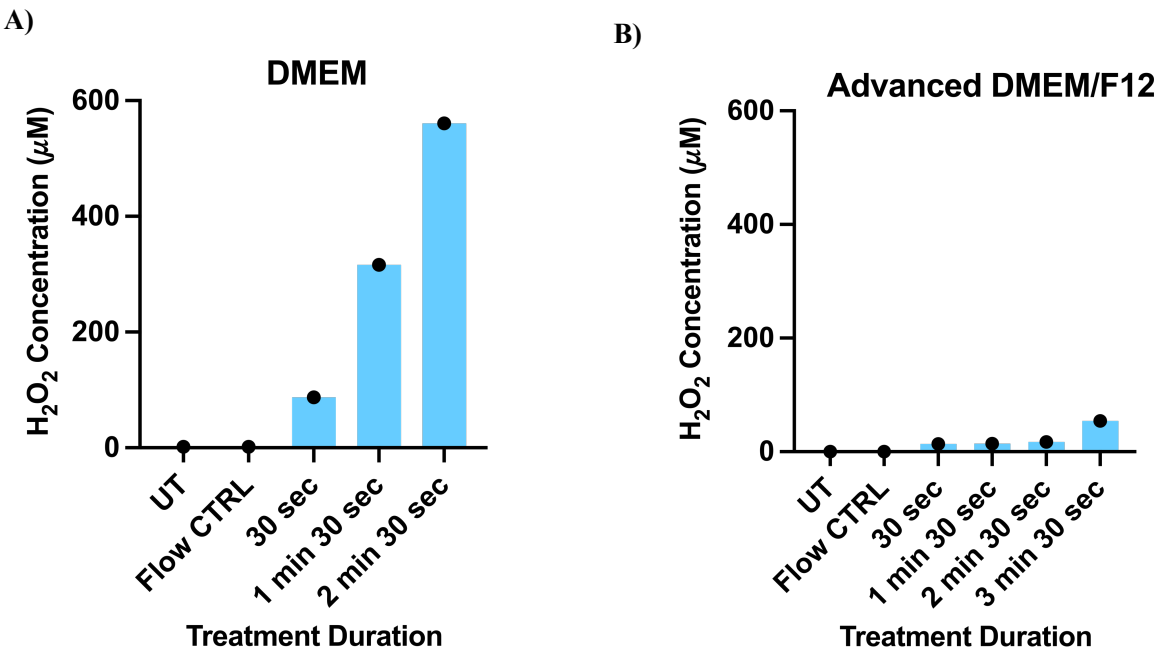

Figure S2. H_2O_2 concentration in DMEM and advanced DMEM/F12 following CAP treatment. H_2O_2 concentrations were measured using a fluorometric assay in DMEM and advanced DMEM/F12 after CAP treatment at four durations (30 sec, 1 min 30 sec, 2 min 30 sec, and 3 min 30 sec) in organoid-free conditions. Data are presented as mean ± SD. Number of biological replicates: $n = 1$ for each condition.